

# Hydrogen Sulfide Protects Human Cardiac Fibroblasts Against H<sub>2</sub>O<sub>2</sub>-induced Injury Through Regulating Autophagy-Related Proteins

Ao Feng<sup>1</sup>, Chen Ling<sup>2</sup>, Lin Xin-duo<sup>3,4</sup>, Wu Bing<sup>3,4</sup>, Wu San-wu<sup>3,4</sup>, Zhan Yu<sup>3,4</sup>, Huang Yu-lan<sup>3,4</sup>, and Zhang You-en<sup>3,4</sup>

Cell Transplantation  
2018, Vol. 27(8) 1222–1234  
© The Author(s) 2018  
Article reuse guidelines:  
sagepub.com/journals-permissions  
DOI: 10.1177/0963689718779361  
journals.sagepub.com/home/cil  


## Abstract

Autophagy, an intracellular bulk degradation process of proteins and organelles, can be induced by myocardial ischemia in the heart. However, the causative role of autophagy in the survival of human cardiac fibroblasts and the underlying mechanisms are incompletely understood. Oxidative stress can induce autophagy in cultured cells upon hydrogen peroxide (H<sub>2</sub>O<sub>2</sub>) exposure. Because hydrogen sulfide (H<sub>2</sub>S) regulates reactive oxygen species (ROS) and apoptosis, we hypothesize that H<sub>2</sub>S may have a cardioprotective function. To examine our hypothesis, we investigated the regulation of autophagy by the H<sub>2</sub>S donor sodium hydrosulfide (NaHS), using a cell model of human cardiac fibroblasts from adult ventricles (HCF-av) that suffered from endoplasmic reticulum (ER) stress by H<sub>2</sub>O<sub>2</sub>. In the present study, we found that the apoptosis and autophagy were induced along with ER stress by H<sub>2</sub>O<sub>2</sub> in the primary cultured HCF-av cells. In contrast, H<sub>2</sub>S suppressed HCF-av cell apoptosis and autophagic flux, in part directly by inhibiting ROS production and preserving mitochondrial functions.

## Keywords

autophagy, cardiac fibroblasts, hydrogen sulfide, lysosome, endoplasmic reticulum

## Introduction

The normal heart is a highly organized structure comprising four major cell types: cardiomyocytes (CMs), cardiac fibroblasts (CFs), endothelial cells (ECs), and vascular smooth muscle cells (VSMCs)<sup>1</sup>. The proportion of each cell type varies in different species, but overall CFs occupy the myocardium predominantly, accounting for approximately two-thirds of the cell populations. CFs synthesize and organize collagens, fibronectins, and other interstitial components to maintain cardiac integrity during physiologic proliferation and extracellular matrix (ECM) turnover, as well as cardiac remodeling. Because the adult mammalian heart has a negligible regenerative capacity, cardiac injury provides a great challenge for the reparative mechanisms after the loss of CMs, resulting in the formation of a collagen-based scar. Due to their abundance, CFs play an important role during normal and pathologic wound healing following myocardial ischemia, heart failure, and atrial fibrillation<sup>2,3</sup>. Therefore, fibroblasts represent an attractive therapeutic candidate for heart disease.

Autophagy is a dynamic process of intracellular bulk degradation. The cytosolic proteins and organelles are

sequestered into double-membrane vesicles, called autophagosomes, to be fused with lysosomes for degradation<sup>4</sup>. Primarily, autophagy is a survival mechanism that allows a starving cell or a cell deprived of growth factors to survive. Theoretically, autophagy serves to regulate protein and organelle abundance and quality. Autophagy occurs at basal levels in the normal condition but is substantially increased in

<sup>1</sup> Department of Medical Imaging Center, Renmin Hospital, Hubei University of Medicine, Shiyan, China

<sup>2</sup> Department of Cardiology, Jinzhou Medical University, Shiyan, China

<sup>3</sup> Institute of Clinical Medicine, Renmin Hospital, Hubei University of Medicine, Shiyan, China

<sup>4</sup> Department of Cardiology, Renmin Hospital, Hubei University of Medicine, Shiyan, China

Submitted: January 9, 2018. Revised: April 21, 2018.

Accepted: April 27, 2018.

## Corresponding Authors:

Huang Yu-lan and You-en Zhang, Institute of Clinical Medicine and Department of Cardiology, Renmin Hospital, Hubei University of Medicine, No.39 Chaoyang Road, Shiyan 442000, China.

Emails: 357875786@qq.com (H. Yu-lan); zye112@hotmail.com (Y. Zhang)



several heart diseases, such as acute and chronic ischemia, heart failure, and cardiac hypertrophy<sup>5–7</sup>. Furthermore, nutritional status, hormonal factors, and other conditions like temperature, oxygen concentration, and cell density are also involved in autophagy regulation<sup>8,9</sup>.

Although H<sub>2</sub>S has been considered as a noxious gas with wide-ranging cytotoxic effects, the accumulating scientific evidence shows that H<sub>2</sub>S plays a pivotal role in cellular signaling and functions, similar to nitric oxide (NO) and carbon monoxide (CO). Our previous preliminary study found that the exogenous H<sub>2</sub>S donor, sodium hydrosulfide (NaHS), has potent anti-inflammatory effects in a heart that has suffered from acute myocardial infarction *in vivo*, which may be in part due to the limitation of the recruitment of CD11b<sup>+</sup>Gr-1<sup>+</sup> myeloid cells<sup>10,11</sup>. Moreover, we also investigated whether NaHS prevented TGF- $\beta$ 1-induced proliferation, migration, regulation of cell growth, transformation to myofibroblasts, and collagen synthesis in human cardiac fibroblasts-to-myofibroblasts assay<sup>12</sup>. Despite the importance of fibroblasts in cardiac pathologies, the direct effects of exogenous H<sub>2</sub>S on autophagy in human CFs upon oxidative stress have not been well elucidated. In the present study, we attempted to determine whether the exogenous H<sub>2</sub>S protected human cardiac fibroblasts-adult ventricular (HCF-av) against hydrogen peroxide (H<sub>2</sub>O<sub>2</sub>)-induced endoplasmic reticulum (ER) stress. We used this *in vitro* model to mimic the ER stress injury to the heart and focused on apoptosis and autophagy. We found that H<sub>2</sub>S markedly inhibited apoptosis and autophagic flux following ER stress induced by H<sub>2</sub>O<sub>2</sub>, supporting that H<sub>2</sub>S could be used as a new therapeutic reagent for treating oxidative-related diseases.

## Materials and Methods

### Cell Culture

HCF-av cells were obtained from ScienCell Research Laboratories (Cat# 6310, San Diego, USA) and cultured in fibroblast medium (FM) supplemented with 2% fetal bovine serum (FBS), 1% fibroblast growth supplement (FGS), and 1% penicillin/streptomycin solution (P/S) according to the manufacturer's protocol. The cells were maintained in a humidified, 37°C incubator with 5% CO<sub>2</sub> and 95% air. Cells were subcultured when they became more than 90% confluent. Cells were used for all the *in vitro* ER stress induction and treatment, measurement of reactive oxygen species (ROS) production, measurement of mitochondrial membrane potential ( $\Delta\psi$ ), and activity of the lysosomal compartment experiments<sup>12</sup>.

### Animal Study, Transverse Aortic Constriction (TAC) Protocol, and DATS Administration

Male C57BL/6 J mice (10 weeks old) were purchased from the Shanghai Laboratory Animal Center of the Chinese Academy of Science (SLAC, Shanghai, China). Animal care and experimental procedures were approved by the Ethics

Committee on Animal Research of Hubei University of Medicine and the Institutional Animal Care and Use Committee of Cleveland Clinic. The TAC procedure was described previously<sup>13</sup>. Briefly, the mice were anesthetized with an intraperitoneal injection of sodium pentobarbital (50 mg/kg). To create pressure overload of the heart, the chest was opened via minithoracotomy to expose the aortic arch and TAC procedure was performed in 12-week-old mice by placing a 7-0 silk suture around the aortic arch between the brachiocephalic trunk and the left carotid artery. The suture was ligated around a 27-gauge blunt needle and the needle was quickly removed after ligation. Animals that did not survive after the surgeries were excluded from further experiments.

For H<sub>2</sub>S therapy, the diallyl trisulfide (DATS) was obtained from LKT Laboratories (St. Paul, MN, USA) and stored at -20°C before use. The mice were injected intraperitoneally once per day for 12 weeks after TAC with DATS (200  $\mu$ g/kg) or vehicle (1% DMSO). The dose of DATS was used for the mice on the basis of previous experience investigating DATS in murine models of cardiac ischemia/reperfusion injury<sup>13</sup>.

### In Vitro ER Stress Induction and Treatment

The HCF-av cells were cultured in serum-free FM for 16 h before treatment and then were challenged with H<sub>2</sub>O<sub>2</sub> (100  $\mu$ M, Sigma-Aldrich, St. Louis, MO, USA) for 24 h to mimic ER stress injury<sup>14–16</sup> in the presence or absence of the exogenous NaHS (100  $\mu$ M, Sigma-Aldrich). The untreated cells were served as the control group and were used in the following experiments.

### Measurement of ROS Production

For measurement of intracellular ROS, the dihydroethidium (DHE, Sigma-Aldrich) was used to monitor ROS production upon different treatments in accordance with the manufacturer's protocol. Briefly, the subconfluent cells were pre-treated with or without NaHS (100  $\mu$ M) for 30 min and then subjected to H<sub>2</sub>O<sub>2</sub> (100  $\mu$ M) treatment for 24 h. Cells were incubated with the DHE (5  $\mu$ M) at 37°C for 30 min and the fluorescence was observed with a Nikon fluorescence microscope (TE-2000U, Nikon, Melville, NY, USA).

### Measurement of Mitochondrial Membrane Potential ( $\Delta\psi$ )

For measurement of mitochondrial membrane potential (MMP), a mitochondria-specific cationic dye JC-1 (100 nM, Life Technologies, Carlsbad, CA, USA) was used to monitor the MMP under different treatments according to the manufacturer's protocol. Briefly, the HCF-av cells were treated with or without H<sub>2</sub>O<sub>2</sub> and then were incubated with JC-1 for 10 min in pre-warmed culture medium. Subsequently, the cells were washed three times with pre-warmed culture medium and the MMP was observed with

a Nikon fluorescence microscope (TE-2000U, Nikon). Both red and green fluorescence emissions were analyzed after JC-1 staining with Image J software (developed at the National Institutes of Health, Bethesda, MD, USA).

### Activity of the Lysosomal Compartment

LysoTracker Deep Red is an ideal fluorescent acidotropic probe that selectively labels vacuoles with low internal pH. Thus, it can be used to label and track functional lysosomes. Briefly, the cells were treated with H<sub>2</sub>O<sub>2</sub> in the presence or absence of NaHS and were then incubated with the LysoTracker Deep Red (70 nM, Life Technologies) in a pre-warmed medium at 37°C for 30 min. Subsequently, the solution was replaced with fresh medium, and the cells were observed using a fluorescence microscope (TE-2000U, Nikon). The activity and intracellular distribution of cathepsin B, a predominant lysosomal protease, was assessed with Magic Red Cathepsin B Detection Kit (Immunochemistry Technologies, LLC, Bloomington, MN, USA). The cells were stained with MagicRed Cathepsin B substrate for 30 min at 37°C and then washed twice with phosphate buffered saline (PBS). Finally, the cells were stained with DAPI (1 µg/ml, Sigma-Aldrich) for 10 min and observed with a fluorescence microscope (TE-2000U, Nikon).

### Cell Apoptosis Assay

The cell apoptosis was detected with propidium iodide (PI)/Annexin V assay kit (BD Biosciences, San Jose, CA, USA) according to the manufacturer's instruction. Briefly, the cells were washed twice with cold PBS and resuspended in 1 × binding buffer at a concentration of 1 × 10<sup>6</sup> cells/ml. Next, 100 µl cell suspension (1 × 10<sup>5</sup> cells) was transferred to a 1 ml tube and stained with 5 µl FITC-Annexin V reagents for 30 min and then the cells were stained with 10 µl PI for 10 min at room temperature. Finally, 400 µl 1 × binding buffer was added to each tube. Flow cytometry was performed with the FACScanto II flow cytometer (Becton Dickinson, Mountain View, CA, USA) with excitation at 488 nm. Fluorescent emission of FITC was measured at 515–545 nm and that of DNA-PI complexes at 564–606 nm. Cell debris was excluded from the analysis by an appropriate forward light scatter threshold setting. Compensation was used wherever necessary.

### Transmission Electron Microscopy (TEM)

For TEM analysis, the cells were rinsed in PBS and fixed with 2.5% glutaraldehyde in PBS (pH 7.4) for 1 h at 4°C. The cells were washed three times with PBS and then were post-fixed in 1% osmium tetroxide (OsO<sub>4</sub>) with 1% potassium ferricyanide. Next, the cells were washed with PBS and dehydrated in a gradient of alcohol (30%, 50%, 70%, and 90%) before embedding in epon. TEM was performed with a Philips CM10 (Andover, MA, USA) at 80 kV on ultra-thin

sections (100 nm on 200 mesh grids) stained with uranyl acetate and counterstained with lead citrate.

### Western Blot Analysis

Western blot analysis was performed as previously described<sup>10</sup>. Briefly, the cells were washed twice with ice-cold PBS and proteins were extracted using lysis buffer (20 mM Tris, pH 7.4, 150 mM NaCl, 2 mM EDTA, 2 mM EGTA, 1 mM sodium orthovanadate, 50 mM sodium fluoride, 1% Triton X-100, 0.1% SDS, and 100 mM phenylmethylsulfonyl fluoride). The extracted proteins were separated in SDS-polyacrylamide gels and transferred to PVDF membranes (PVDF, Millipore, Burlington Massachusetts, USA). The membranes were washed three times for 10 min each time with TBST and incubated with primary antibodies at 4°C overnight. The primary antibodies used in this study are listed below: activated caspase 3 p17 (Bioworld; 1:1000 dilution Dublin, OH, USA), BiP (Cell Signaling Technology; 1:1000 dilution Danvers, MA, USA), C/EBP homologous protein (CHOP) (Cell Signaling Technology; 1:1000 dilution), LC3 (Sigma-Aldrich; 1:1000 dilution), Beclin1 (Abcam; 1:1000 dilution, Cambridge, UK), P62/SQSTM1 (Cell Signaling Technology; 1:1000 dilution), Puma (Cell Signaling Technology; 1:1000 dilution), and Ubiquitin (Cell Signaling Technology; 1:1000 dilution). The membranes were washed with TBST followed by incubation with indicated horseradish peroxidase (HRP)-conjugated secondary antibodies (Jackson Immunoresearch, West Grove, PA, USA). Detection was performed using enhanced chemiluminescence (ECL) Western blotting detection reagent (G&E) and the data were quantified by densitometry.

**Proteasome activity assay.** Proteasome activity was measured by aminomethylcoumarin (AMC)-linked synthetic peptide substrates: Ac-Gly-Pro-Leu-Asp-AMC and Suc-Leu-Leu-Val-Tyr-AMC (Proteasome Substrate Pack, Enzo Life Sciences, Farmingdale NY, USA). Proteins were extracted from treated or untreated cells with lysis buffer (50 mM HEPES pH 7.5, 5 mM EDTA, 150 mM NaCl, 1% Triton X-100, and 2 mM ATP). Next, 200 µl of lysate containing equal amounts of protein (5 µg) were incubated for 30 min at 37°C in a dark environment with 2.5 µl of each substrate. The reaction was stopped by stop buffer (ice-cold 96% ethanol). The proteasome activity was detected by Tecan Infinite M200 Plate Reader (380 nm excitation and 460 nm emission, Männedorf, Switzerland).

**Statistical analysis.** All experiments were carried out in triplicate under identical conditions and data were represented as means ± standard error of the mean (SEM). For animal studies, experiments were performed in duplicate and each group included three mice. Statistical analysis was performed with SPSS software (IBM Corp., Armonk, NY, USA). Different groups were compared by one-way analysis

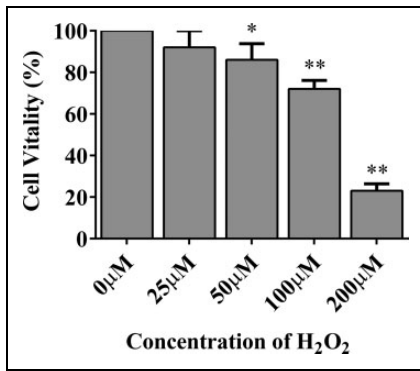


**Figure 1.** The effect of H<sub>2</sub>O<sub>2</sub> on HCF-av cell vitality. The HCF-av cells were treated with different concentrations of H<sub>2</sub>O<sub>2</sub> for 24 h and then the cell vitality was determined by CCK-8 kit ( $n = 3$ ). \* $P < 0.05$ , \*\* $P < 0.01$  vs. control.

of variance (ANOVA), followed by Tukey's or Bonferroni post-hoc test when applicable. Comparisons between the two groups were assessed by the  $t$  test. A  $P$  value less than 0.05 was considered significant.

## Results

### The Effect of H<sub>2</sub>O<sub>2</sub> on Cell Proliferation of HCF-av Cells

HCF-av cells were treated with H<sub>2</sub>O<sub>2</sub> at different concentrations (0–200 μM) for 24 h. Cell vitality was measured by a Cell Counting Kit (CCK-8, Dojindo, Rockville, MD, USA) according to the manufacturer's protocol. H<sub>2</sub>O<sub>2</sub> exhibited cytotoxicity in HCF-av cells in a dose-dependent manner. There was no significant loss of vitality with 0 or 25 μM H<sub>2</sub>O<sub>2</sub> in HCF-av cells. In contrast, decreases of nearly 14%, 28%, and 77% cell

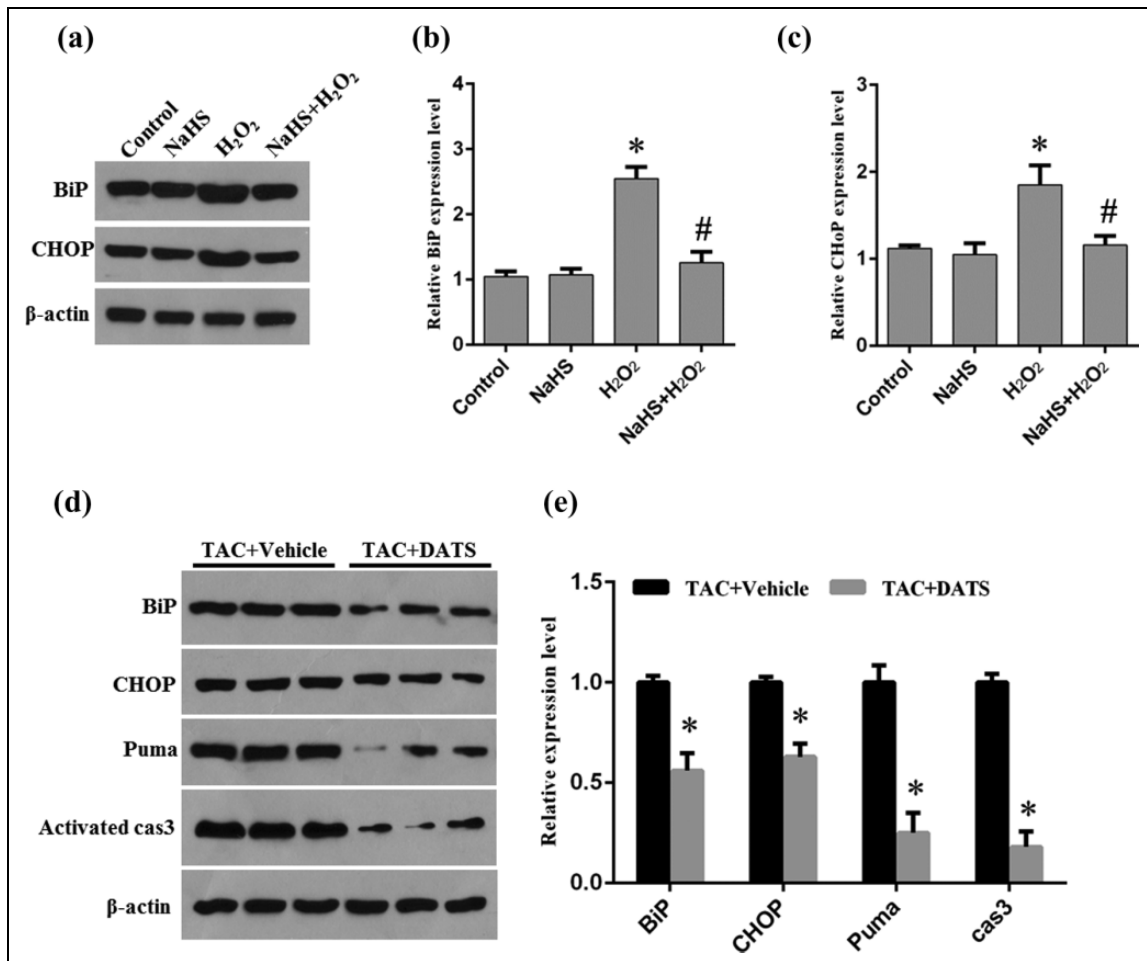


**Figure 2.** H<sub>2</sub>S ameliorates H<sub>2</sub>O<sub>2</sub>-induced ER stress in HCF-av cells. (a) Western blot analysis of HCF-av cells upon different treatments was performed to detect BiP and CHOP. β-actin served as the loading control. (b,c) Quantitative analysis of the changes of BiP and CHOP in treated cells. Data represent mean ± SEM ( $n = 3$ . \* $P < 0.05$  vs. control; # $P < 0.05$  vs. NaHS). (d) Representative Western blot analysis for BiP, CHOP, Puma, and caspase 3 expression in hearts from vehicle- and DATS-treated mice. β-actin served as the loading control. (e) Quantitative analysis of the changes of BiP and CHOP in treated cells. Data represent mean ± SEM ( $n = 3$ . \* $P < 0.05$  vs. TAC + Vehicle).

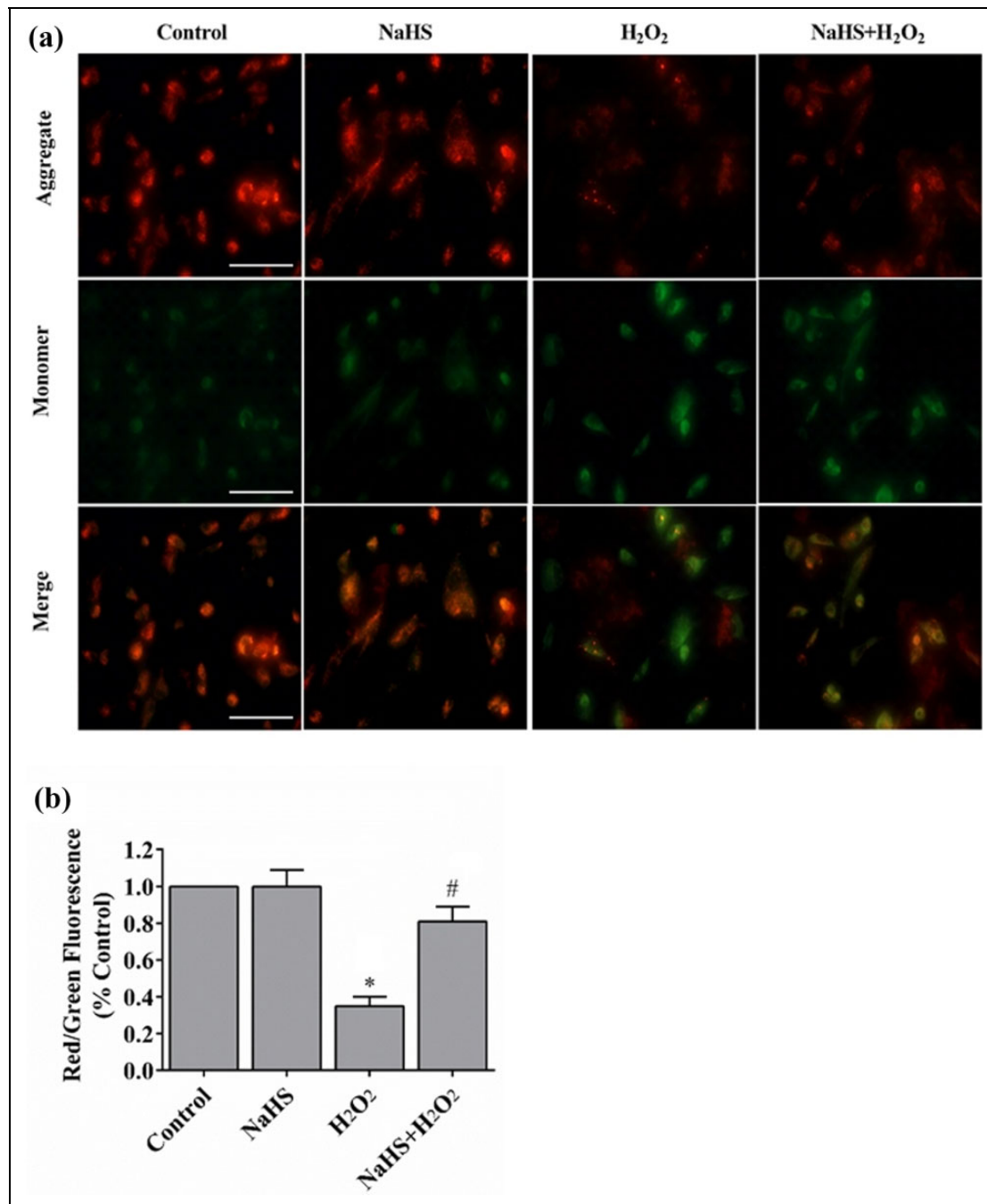


**Figure 3.** H<sub>2</sub>S restores H<sub>2</sub>O<sub>2</sub>-induced reduction of  $\Delta\psi$ . (a) The  $\Delta\psi$  loss was determined by the lipophilic cationic probe JC-1. Red signal indicated JC-1 in mitochondria. Green signal indicated cytosolic JC-1. Magnification,  $\times 400$ . (b) Quantitative analysis of membrane potential ( $n = 3$ ). \* $P < 0.01$  vs. control; # $P < 0.01$  vs. NaHS; # $P < 0.01$  vs. H<sub>2</sub>O<sub>2</sub>.

vitality occurred in HCF-av cells exposed to 50  $\mu$ M, 100  $\mu$ M, and 200  $\mu$ M H<sub>2</sub>O<sub>2</sub> for 24 h, respectively (Figure 1). Therefore, we used 100  $\mu$ M H<sub>2</sub>O<sub>2</sub> for the next experiments.

### H<sub>2</sub>S Reduces ER Stress Induced by H<sub>2</sub>O<sub>2</sub> and TAC

The ER stress was induced by H<sub>2</sub>O<sub>2</sub> in cultured HCF-av cells, which was assessed by the ER stress protein markers

immunoglobulin binding protein (BiP) and CHOP. H<sub>2</sub>O<sub>2</sub> challenge provoked a significantly increased Expression of BiP and CHOP compared with the control cells (Figure 2(a–c)). Interestingly, H<sub>2</sub>S treatment effectively abrogated ER stress by reducing the expression levels of BiP and CHOP induced by H<sub>2</sub>O<sub>2</sub>. To further confirm our results, we evaluated the effects of H<sub>2</sub>S on the ER stress in heart tissues from mice after TAC. As shown in Figure 2(d,e), the ER

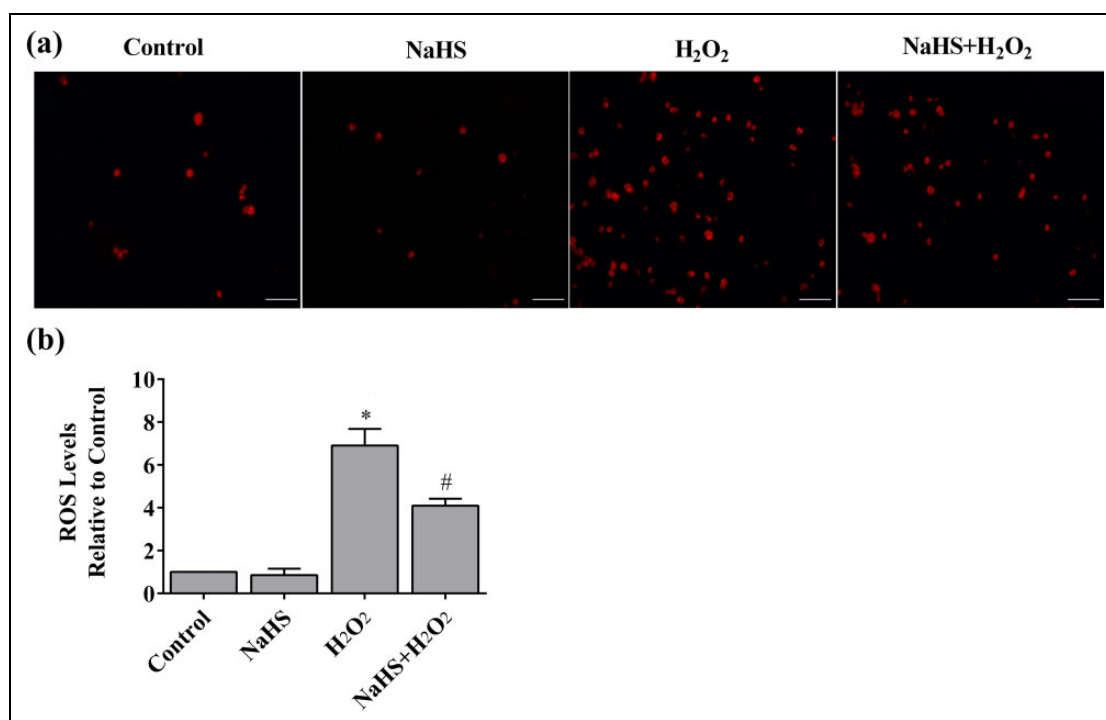


**Figure 4.** H<sub>2</sub>S suppresses superoxide anion production induced by H<sub>2</sub>O<sub>2</sub>. (a) Intracellular superoxide anion production was detected with dihydroethidium and observed by fluorescent microscopy. (b) The fluorescent signal was measured and quantified ( $n = 6$ ). \* $P < 0.01$  vs. control; # $P < 0.01$  vs. NaHS; # $P < 0.01$  vs. H<sub>2</sub>O<sub>2</sub>.

stress-related markers (BiP, CHOP, and Puma) and caspase-3 were significantly induced by TAC. Strikingly, BiP, CHOP, Puma, and caspase-3 was markedly reduced by H<sub>2</sub>S after TAC. Altogether, these results demonstrate that H<sub>2</sub>S protected heart cells against ER stress.

### H<sub>2</sub>S Prevents Loss of MMP Induced by H<sub>2</sub>O<sub>2</sub>

Mitochondrial function is highly susceptible to oxidative damage. Therefore, we investigated whether H<sub>2</sub>S protected mitochondria from H<sub>2</sub>O<sub>2</sub>-induced ER stress. Mitochondria in control cells stained with JC-1 exhibited bright orange fluorescence. However, when cells were exposed to H<sub>2</sub>O<sub>2</sub>, they showed fewer and less intense JC-1 fluorescence in mitochondria (Figure 3(a)), which was greatly improved by pretreatment of H<sub>2</sub>S (Figure 3(b)). These results suggested that H<sub>2</sub>S could prevent the loss of mitochondrial  $\Delta\psi$  upon oxidative stress.

### H<sub>2</sub>S Suppresses ROS Production Induced by H<sub>2</sub>O<sub>2</sub>

To determine the effect of H<sub>2</sub>S on H<sub>2</sub>O<sub>2</sub>-induced ROS production from ER and mitochondria, DHE, a specific fluorescent probe for O<sub>2</sub><sup>-</sup>, was used to track cellular ROS generation (Figure 4(a)). HCF-av cells were subjected to H<sub>2</sub>O<sub>2</sub> treatment and ROS production was significantly enhanced compared with the control. Conversely, this elevation was markedly suppressed by pretreatment of cells with H<sub>2</sub>S (Figure 4(a,b)). No significant difference in ROS

production was observed with NaHS treatment alone. These results indicated that H<sub>2</sub>S abrogated ROS production in HCF-av cells.

### H<sub>2</sub>S Attenuate Cell Apoptosis Induced by H<sub>2</sub>O<sub>2</sub>

ROS production is known to promote apoptosis. To evaluate the effect of H<sub>2</sub>S on ER stress-induced apoptosis, HCF-av cells were subjected to different treatments and the cell death was analyzed by flow cytometry. As shown in Figure 5(a,b), oxidative stress induced by H<sub>2</sub>O<sub>2</sub> resulted in significant cell death (Annexin V<sup>+</sup>/PI<sup>+</sup> cells) compared with the control cells. By contrast, pretreatment of NaHS dramatically reduced cell death induced by H<sub>2</sub>O<sub>2</sub>. These results were consistent with the level of activated caspase 3, a cell apoptotic marker (Figure 5(c,d)).

### H<sub>2</sub>S Ameliorates Lysosomal Activity in HCF-av Cells Induced by H<sub>2</sub>O<sub>2</sub>

To investigate the role of lysosomal activity on cell apoptosis and damage of ER or mitochondria, HCF-av cells were subjected to different treatments and then incubated with LysoTracker Deep Red, which labeled the highly acidic lysosomal vacuoles and monitored activity of the vacuolar H<sup>+</sup>-ATPase (v-ATPase). We found that H<sub>2</sub>O<sub>2</sub> exposure markedly increased the LysoTracker red staining. However,

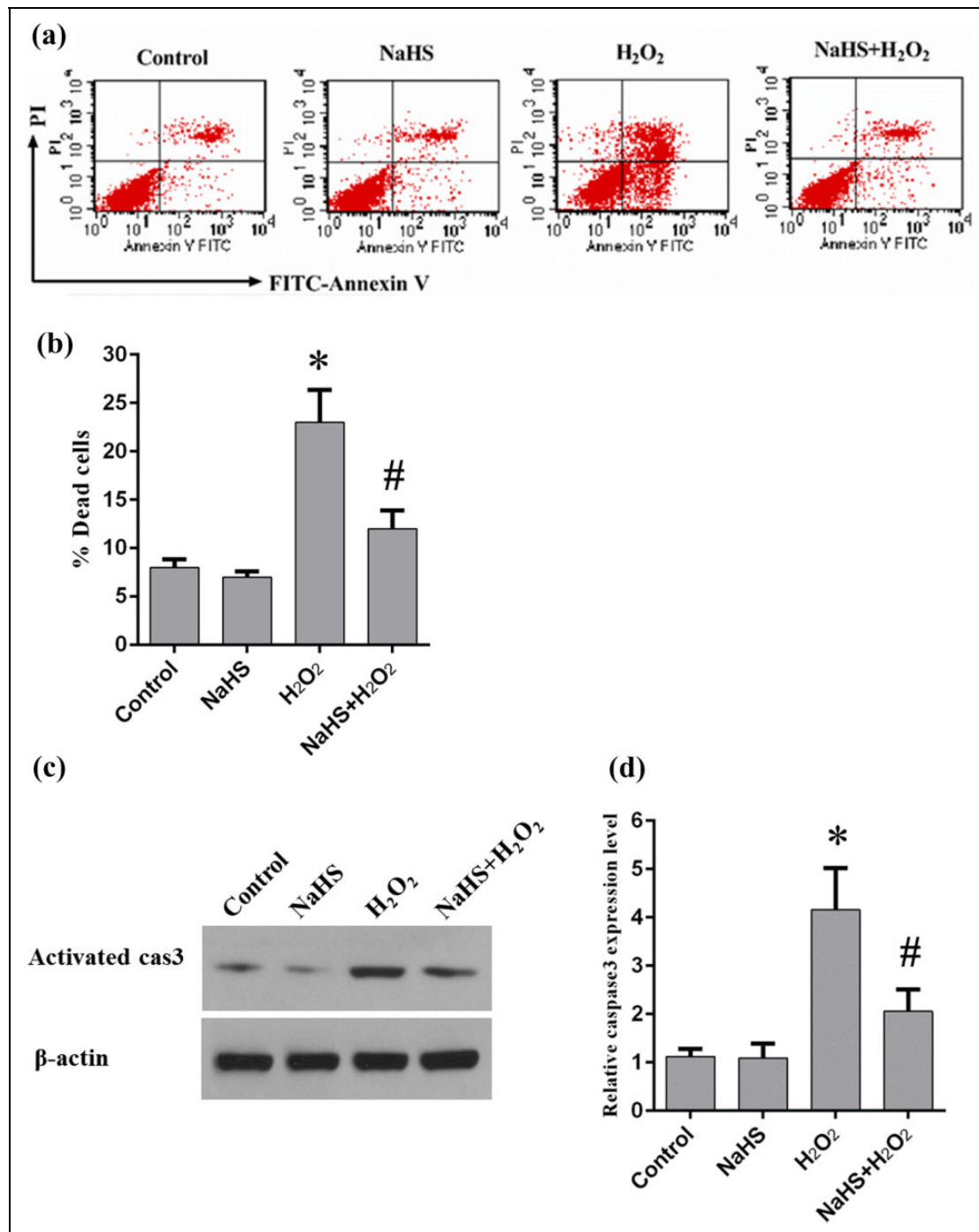


**Figure 5.** H<sub>2</sub>S attenuates cell apoptosis in HCF-av cells induced by H<sub>2</sub>O<sub>2</sub>. Cell death analysis of treated cells was performed by flow cytometry with Annexin V/PI double staining (a,b). Representative images and quantitative analysis were shown in (c) and (d), respectively. Data represent mean  $\pm$  SEM ( $n = 3$ ; \* $P < 0.05$  vs. control cells, # $P < 0.05$  vs. indicated cells).

this fluorescent signal was significantly decreased by pre-treatment of NaHS (Figure 6(a,b)).

### H<sub>2</sub>S Prevents H<sub>2</sub>O<sub>2</sub>-Induced Autophagy

To investigate whether the autophagy was activated in the period following increased lysosomal activity in HCF-av

cells undergoing oxidative stress, the expression level of cathepsin B was examined using Magic Red staining. As shown in Figure 7(a), H<sub>2</sub>O<sub>2</sub>-induced ER stress caused approximately three-fold increase in fluorescence intensity of cathepsin B in HCF-av cells compared to the control cells. Consistent with this finding, cells treated with H<sub>2</sub>O<sub>2</sub> displayed an increased abundance of multilamellar

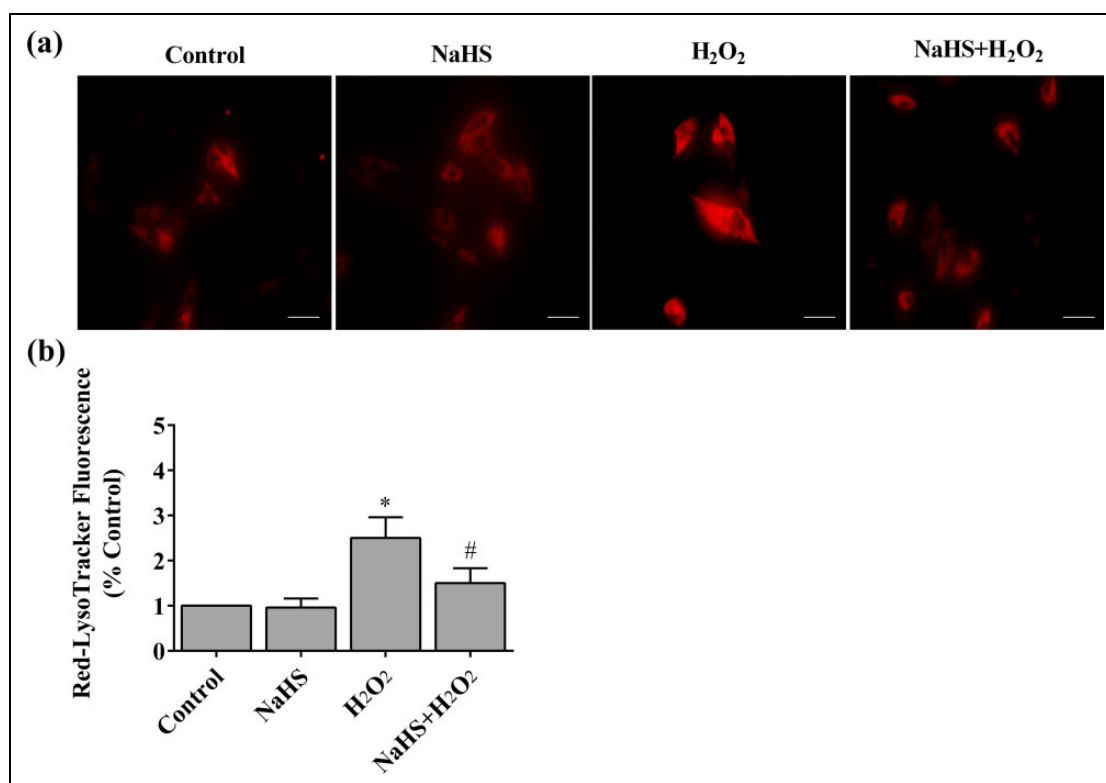


**Figure 6.** H<sub>2</sub>S ameliorates lysosomal activity in HCF-av cells induced by H<sub>2</sub>O<sub>2</sub>. (a) Cells were subjected to different treatments and then stained with 70 nM LysoTracker<sup>®</sup> Deep Red (magnification,  $\times 400$ ). (b) The fluorescent signal (red) was measured and quantified ( $n = 6$ ). \* $P < 0.01$  vs. control; # $P < 0.01$  vs. NaHS; # $P < 0.01$  vs. H<sub>2</sub>O<sub>2</sub>.

autophagosomes (Figure 7(b)). Strikingly, these phenomena were significantly diminished when the cells were treated with NaHS (Figure 7(c,d)).

### H<sub>2</sub>S Regulates the Expression of LC3-II, Beclin1, and P62 During Autophagy

The expression levels of LC3-I/II, Beclin1, and P62 play vital roles for autophagic activity<sup>17–19</sup>. To further investigate the role of H<sub>2</sub>S-regulated autophagy induced by H<sub>2</sub>O<sub>2</sub>, HCF-av cells were subjected to different treatments and the autophagy-related proteins were detected. As shown in Figure 8(a), the expression levels of Beclin1, LC3-II/LC-I ratio, and P62 were robustly increased when cells were treated with H<sub>2</sub>O<sub>2</sub>. Meanwhile, the increases of these key proteins were diminished in cells pretreated with H<sub>2</sub>S (Figure 8(a–d)). Because p62 plays a key role in both autophagy and the ubiquitin proteasome system, we further investigate the effects of H<sub>2</sub>S on the ubiquitin proteasome system upon H<sub>2</sub>O<sub>2</sub> treatment in HCF-av cells. As shown in Figure 8(e–g), the proteasome activity and ubiquitin expression did not change when cells were treated with or without H<sub>2</sub>S plus H<sub>2</sub>O<sub>2</sub>. These results suggested that H<sub>2</sub>S could regulate the autophagic activity but not proteasome activity in HCF-av cells under H<sub>2</sub>O<sub>2</sub> treatment.

### Discussions

Recent studies indicated that H<sub>2</sub>S was a powerful endogenous second messenger, capable of modulating a variety of physiological or pathophysiological events in mammalian cells and tissues<sup>20,21</sup>. These results prompted us to investigate the potential role of H<sub>2</sub>S as a cardioprotective reagent. Previous studies indeed suggest that H<sub>2</sub>S was a potent cardioprotective signaling molecule reagent for heart disease<sup>22,23</sup>. Current studies have shown that H<sub>2</sub>S can regulate the activation of ion channel, and upregulate antioxidant, anti-apoptotic, and anti-inflammatory signaling pathways<sup>10,24–26</sup>. In the present study, we evaluated effects of NaHS on the *in vitro* ER stress cell model. H<sub>2</sub>O<sub>2</sub> is one kind of ROS and has been widely used in experiments to mimic the situation of oxidative stress. Different concentrations of H<sub>2</sub>O<sub>2</sub> have been widely used in different cell types, and different cell types have showed different responses to oxidative stress induced by H<sub>2</sub>O<sub>2</sub><sup>27</sup>. In the present study, the HCF-av cells were exposed to H<sub>2</sub>O<sub>2</sub> to mimic *in vivo* ER stress. BiP expression level was robustly increased, which revealed ER stress induced by H<sub>2</sub>O<sub>2</sub> in HCF-av cells (Figure 2). This result is consistent with the accumulation of CHOP (also known as growth-arrest and DNA damage inducible gene 153) in HCF-av cells induced by H<sub>2</sub>O<sub>2</sub>, which was a transcription factor and activated at multiple levels during ER

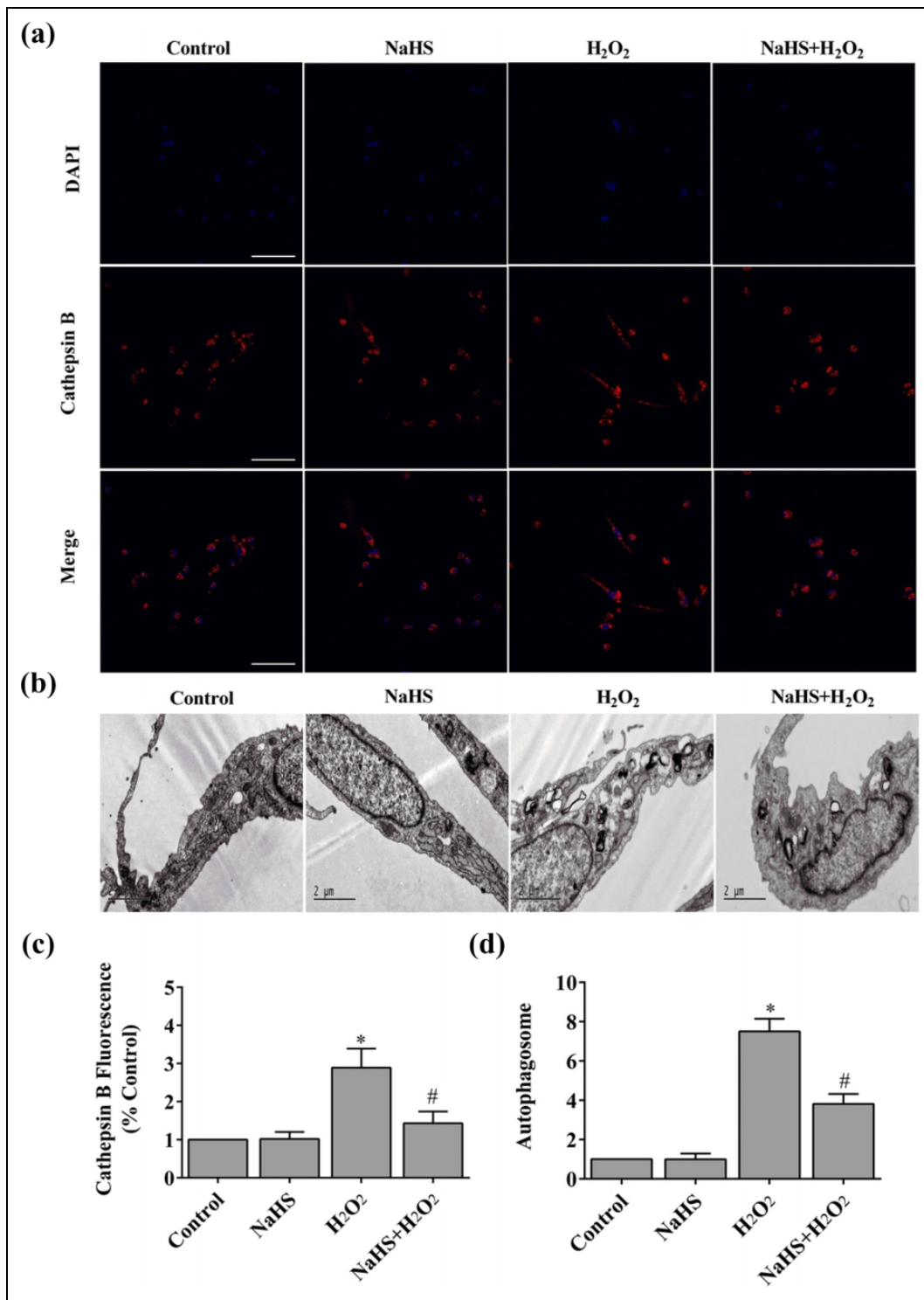


**Figure 7.** H<sub>2</sub>S blocks autophagy in HCF-av cells induced by H<sub>2</sub>O<sub>2</sub>. (a) Cells were subjected to different treatments and then stained with Magic Red<sup>®</sup> Cathepsin B Detection Kit (magnification, ×200). (b) Representative TEM micrographs upon H<sub>2</sub>O<sub>2</sub> treatment. (c) The fluorescence (red) intensity of cathepsin B was measured and quantified (n = 6). (d) Quantification of the autophagosome (n = 4). \*P < 0.01 vs. control; #P < 0.01 vs. NaHS; #P < 0.05 vs. H<sub>2</sub>O<sub>2</sub>.

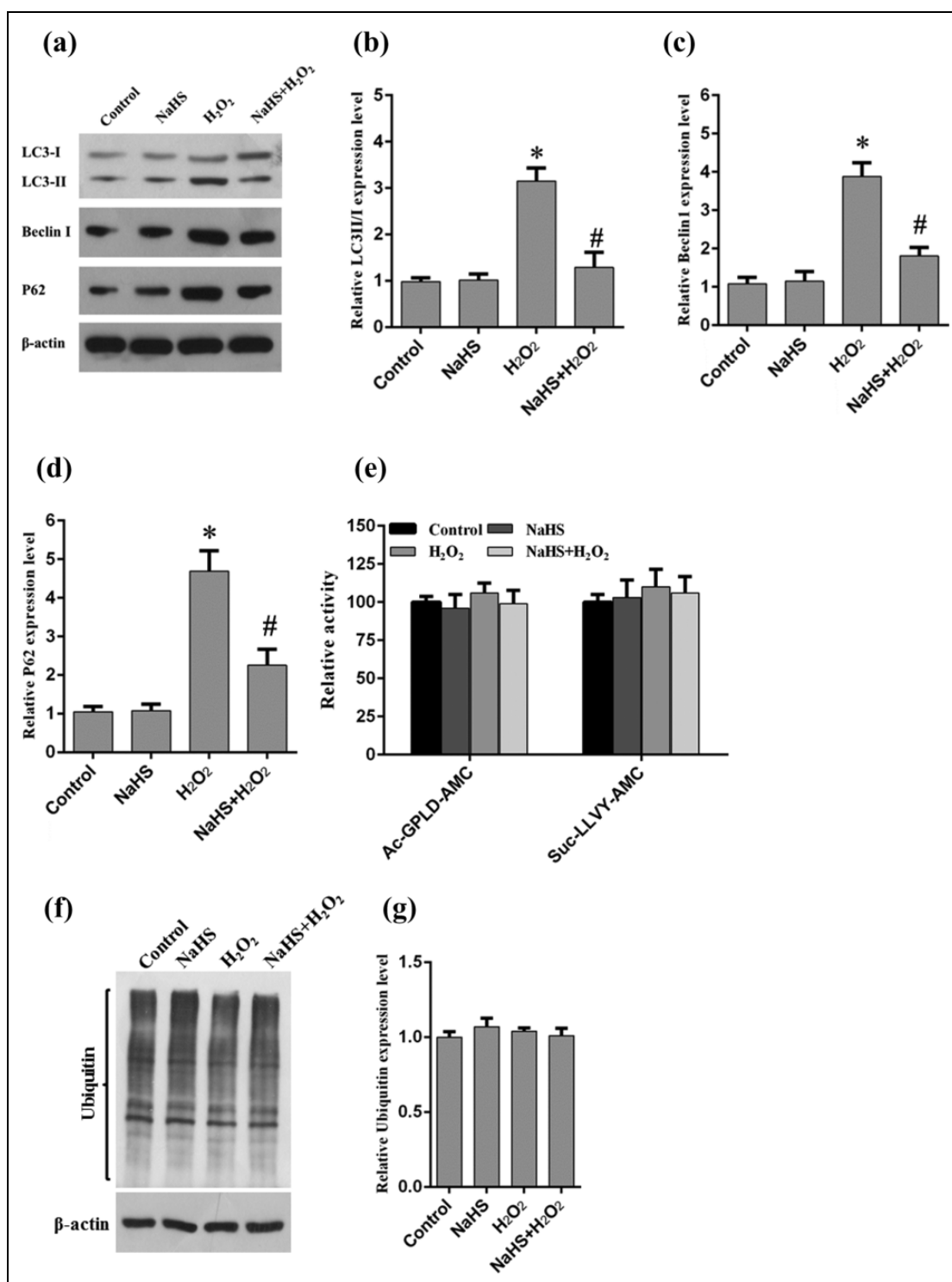


**Figure 8.** H<sub>2</sub>S regulates the expression of LC3-II, Beclin I, and P62 during autophagy. (a) Western blot analysis of HCF-av cells upon different treatments was performed to detect LC3I/II, Beclin I, and P62. (b–d) Quantitative analysis of the changes of LC3I/II, Beclin I, and P62 in treated cells ( $n = 3$ ). \* $P < 0.01$  vs. control; \* $P < 0.01$  vs. NaHS; # $P < 0.05$  vs. H<sub>2</sub>O<sub>2</sub>. (e) Proteasome activity was measured using AMC-linked substrate peptides under different treatments ( $n = 3$ ). (f) Representative Western blot analysis for ubiquitin expression.  $\beta$ -actin served as the loading control. (g) Quantitative analysis of the changes of ubiquitin in treated cells ( $n = 3$ ).

stress<sup>28–30</sup>. Because ER stress is closely related to cell apoptosis, we have found that ER stress significantly elevated the activated caspase 3 level in HCF-av cells induced by H<sub>2</sub>O<sub>2</sub> (Figure 5). Importantly, the activated caspase 3 level is abrogated by H<sub>2</sub>S treated HCF-av cells induced by H<sub>2</sub>O<sub>2</sub>.

Mitochondria played pivotal roles in the two types of cell death: apoptosis and necrosis<sup>31</sup>. However, autophagy, a cellular stress response, is involved in a variety of diseases and has recently been proposed as a third distinct mode of cell death. Autophagy is a dynamic process involving the rearrangement of subcellular membranes to sequester cytoplasm and organelles which are delivered to the lysosome or vacuole, and then the sequestered cargo is degraded and recycled<sup>4</sup>. Accumulated evidence indicates that autophagy may constitute an important physiological response to cardiac stresses, ischemia, or pressure overload, which are frequently encountered in patients with coronary artery disease, hypertension, aortic valvular disease, and congestive heart failure. The accumulation of autophagosomes has been noted in cardiac biopsy tissues of patients with these disorders, rodent models of these cardiac diseases, and isolated stressed cardiomyocytes<sup>4</sup>. Autophagy participated in the constitutive turnover of mitochondria in oxidative tissues, and removal of damaged organelles<sup>32,33</sup>. One of the conclusions of our study is that the protective mechanism of H<sub>2</sub>S may be involved in stabilization of the mitochondria in H<sub>2</sub>O<sub>2</sub>-induced cell death. Changes of the mitochondrial permeability transition (MPT) and loss of  $\Delta\psi$  triggered autophagic scavenging. Our findings suggested that H<sub>2</sub>O<sub>2</sub> exposure reduced JC-1 aggregates in HCF-av cells, indicating mitochondria  $\Delta\psi$  was decreased. Conversely, pretreatment of H<sub>2</sub>S restored the mitochondria  $\Delta\psi$  induced by H<sub>2</sub>O<sub>2</sub>. Furthermore, autophagic flux was significantly increased following H<sub>2</sub>O<sub>2</sub> exposure, as shown by the multilamellar autophagosomes and the increased LC3-II/LC3-I ratio, Beclin1, and p62 protein level. In contrast, exogenous H<sub>2</sub>S completely abrogates these phenomena.

In eukaryotic cells, the lysosome is a major organelle that contains a lot of enzymes, which can degrade essentially any subcellular component by hydrolases such as proteins, lipids, nucleic acids, and carbohydrates<sup>34</sup>. Lysosomal enzymes also play a role in the activation of certain types of caspase, which are involved in cell apoptosis. Lysosomes have been referred to as “suicide bags,” as they contribute to autophagic cell death<sup>35,36</sup>. Moreover, ROS can induce lysosomal permeabilization before mitochondrial dysfunction. Although oxidative stress induces many alterations within the cell, mitochondria may be the first organelle to be demerged by ROS. Lysosomal enzymes have been found to act on mitochondria and promote mitochondrial ROS generation, creating a feedback loop and leading to more lysosomal permeabilization. Our studies determined the effect of H<sub>2</sub>S on the autophagic activity induced by H<sub>2</sub>O<sub>2</sub>. Autophagy was involved in the delivery of autophagosomes and their contents to lysosomes and accomplished the catabolic processes of autophagy. We found that cellular

lysosomal activation and the expression level of cathepsin B are both increased in cells with ER stress induced by H<sub>2</sub>O<sub>2</sub>, but are diminished by NaHS treatment.

Recent studies have shown that H<sub>2</sub>S is a strong promoter of angiogenesis<sup>37,38</sup> and stimulates cell replication, migration, and tube formation<sup>39</sup>. Furthermore, H<sub>2</sub>S also promotes angiogenesis *in vivo*<sup>40</sup> and the proangiogenic effects of H<sub>2</sub>S on chronic vascular disease have been reported<sup>39</sup>. However, the protective role of H<sub>2</sub>S in ER stress and autophagy induced by oxidative stress in the heart is still obscure. A previous study reported that H<sub>2</sub>S attenuates oxidative stress in the heart through activation of nuclear factor E2-related factor (Nrf2)<sup>41</sup>, because Nrf2 regulates a large number of gene expressions for enzymes that serve to detoxify pro-oxidative stressors<sup>42</sup>, such as GPx1 and HO-1, via binding to the antioxidant response element found in the gene's promoter region<sup>40</sup>. Maybe that is why H<sub>2</sub>S can prevent ER stress, autophagy, and heart cell apoptosis induced by H<sub>2</sub>O<sub>2</sub>. In the current study we demonstrated that H<sub>2</sub>S treatment dramatically repressed ER stress marker and autophagy marker expression and cell apoptosis induced by H<sub>2</sub>O<sub>2</sub> using an *in vitro* model (HCF-av cells). Furthermore, the *in vivo* model also suggested that ER stress-related markers and heart cell apoptosis were significantly blocked by H<sub>2</sub>S treatment (Figure 2(d)). Further investigations are needed to determine the precise mechanism by which H<sub>2</sub>S prevents ER stress, autophagy, and cell apoptosis induced by oxidative stress in the heart.

In summary, H<sub>2</sub>S pretreatment efficiently protects HCF-av cells from H<sub>2</sub>O<sub>2</sub>-induced ER stress, apoptosis, and autophagy, which maintains mitochondria membrane integrity and prevents the activation of caspase 3. Our study suggests that H<sub>2</sub>S could potentially be a therapeutic reagent for suppressing ER stress in the heart.

### Author Contributions

Ao Feng and Chen Ling contributed equally to this work.

### Ethical Approval

Animal care and experimental procedures were approved by the Ethics Committee on Animal Research of Hubei University of Medicine and the Institutional Animal Care and Use Committee of Cleveland Clinic.

### Statement of Human and Animal Rights

Male C57BL/6 J mice (10 weeks old) were purchased from the Shanghai Laboratory Animal Center of the Chinese Academy of Science (SLAC, Shanghai, China).

### Statement of Informed Consent

Statement of Informed Consent is not applicable for this article.

### Declaration of Conflicting Interests

The authors declared no potential conflicts of interest with respect to the research, authorship, and/or publication of this article.

## Funding

The authors disclosed receipt of the following financial support for the research, authorship, and/or publication of this article: This study was supported by the National Nature Science Foundation of China (No. 81500237) and Special Foundation for Knowledge Innovation of Hubei Province (Nature Science Foundation) (No. 2017CFB563).

## References

- Fan D, Takawale A, Lee J, Kassiri Z. Cardiac fibroblasts, fibrosis and extracellular matrix remodeling in heart disease. *Fibrogenesis Tissue Repair*. 2012;5(1):15.
- Cunnington RH, Wang B, Ghavami S, Bathe KL, Rattan SG, Dixon IM. Antifibrotic properties of c-Ski and its regulation of cardiac myofibroblast phenotype and contractility. *Am J Physiol Cell Physiol*. 2011;300(1):C176–C186.
- Becher PM, Gotzhein F, Klingel K, Escher F, Blankenberg S, Westermann D, Lindner D. Cardiac function remains impaired despite reversible cardiac remodeling after acute experimental viral myocarditis. *J Immunol Res*. 2017;6590609. doi: 10.1155/2017/6590609
- Levine B, Kroemer G. Autophagy in the pathogenesis of disease. *Cell*. 2008;132(1):27–42.
- Cao DJ, Wang ZV, Battiprolu PK, Jiang N, Morales CR, Kong Y, Rothermel BA, Gillette TG, Hill JA. Histone deacetylase (HDAC) inhibitors attenuate cardiac hypertrophy by suppressing autophagy. *Proc Natl Acad Sci USA*. 2011;108(10):4123–4128.
- Ma X, Liu H, Foyil SR, Godar RJ, Weinheimer CJ, Hill JA, Diwan A. Impaired autophagosome clearance contributes to cardiomyocyte death in ischemia/reperfusion injury. *Circulation*. 2012;125(25):3170–3181.
- Pistoia V, Pezzolo A. Involvement of HMGB1 in resistance to tumor vessel-targeted, monoclonal antibody-based immunotherapy. *J Immunol Res*. 2016;3142365. doi: 10.1155/2016/3142365
- Klionsky DJ. Autophagy: from phenomenology to molecular understanding in less than a decade. *Nat Rev Mol Cell Biol*. 2007;8(11):931–937.
- Maiuri MC, Zalckvar E, Kimchi A, Kroemer G. Self-eating and self-killing: crosstalk between autophagy and apoptosis. *Nat Rev Mol Cell Biol*. 2007;8(9):741–752.
- Zhang Y, Li H, Zhao G, Sun A, Zong NC, Li Z, Zhu H, Zou Y, Yang X, Ge J. Hydrogen sulfide attenuates the recruitment of cd11b(+)-gr-1(+) myeloid cells and regulates bax/bcl-2 signaling in myocardial ischemia injury. *Sci Rep*. 2014;4:4774.
- Wu T, Li H, Wu B, Zhang L, Wu SW, Wang JN, Zhang YE. Hydrogen sulfide reduces recruitment of cd11b+gr-1+ cells in mice with myocardial infarction. *Cell Transplant*. 2017;26(5):753–764.
- Zhang Y, Wang J, Li H, Yuan L, Wang L, Wu B, Ge J. Hydrogen sulfide suppresses transforming growth factor-beta1-induced differentiation of human cardiac fibroblasts into myofibroblasts. *Sci China Life Sci*. 2015;58(11):1126–1134.
- Polhemus D, Kondo K, Bhushan S, Bir SC, Kevil CG, Murohara T, Lefer DJ, Calvert JW. Hydrogen sulfide attenuates cardiac dysfunction after heart failure via induction of angiogenesis. *Circ Heart Fail*. 2013;6(5):1077–1086.
- Anderson KJ, Russell AP, Foletta VC. Ndr2 promotes myoblast proliferation and caspase 3/7 activities during differentiation, and attenuates hydrogen peroxide – but not palmitate-induced toxicity. *FEBS Open Bio*. 2015;7(5):668–681.
- Zhu Y, Zhao KK, Tong Y, Zhou YL, Wang YX, Zhao PQ, Wang ZY. Exogenous NAD(+) decreases oxidative stress and protects H<sub>2</sub>O<sub>2</sub>-treated RPE cells against necrotic death through the up-regulation of autophagy. *Sci Rep*. 2016;5(6):26322.
- Philip L, Shivakumar K. cIAP-2 protects cardiac fibroblasts from oxidative damage: an obligate regulatory role for ERK1/2 MAPK and NK-kappaB. *J Mol Cell Cardiol*. 2013;9(62):217–226.
- Pattingre S, Tassa A, Qu X, Garuti R, Liang XH, Mizushima N, Packer M, Schneider MD, Levine B. Bcl-2 antiapoptotic proteins inhibit Beclin 1-dependent autophagy. *Cell*. 2005;122(6):927–939.
- Kabeya Y, Mizushima N, Ueno T, Yamamoto A, Kirisako T, Noda T, Kominami E, Ohsumi Y, Yoshimori T. LC3, a mammalian homologue of yeast Apg8p, is localized in autophagosomal membranes after processing. *EMBO J*. 2000;19(21):5720–5728.
- Kanamori H, Takemura G, Goto K, Maruyama R, Tsujimoto A, Ogino A, Takeyama T, Kawaguchi T, Watanabe T, Fujiwara T, Fujiwara H, Seishima M, Minatoguchi S. The role of autophagy emerging in postinfarction cardiac remodeling. *Cardiovasc Res*. 2011;91(2):330–339.
- Greabu M, Totan A, Miricescu D, Radulescu R, Virlan J, Calenic B. Hydrogen sulfide, oxidative stress and periodontal diseases: a concise review. *Antioxidants*. 2016;5(1):1–13.
- Sun J, Aponte AM, Menazza S, Gucek M, Steenbergen C, Murphy E. Additive cardioprotection by pharmacological post-conditioning with hydrogen sulfide and nitric oxide donors in mouse heart: S-sulfhydration vs. S-nitrosylation. *Cardiovasc Res*. 2016;110(1):96–106.
- Predmore BL, Lefer DJ. Hydrogen sulfide-mediated myocardial pre- and post-conditioning. *Expert Rev Clin Pharmacol*. 2011;4(1):83–96.
- Ma SF, Luo Y, Ding YJ, Chen Y, Pu SX, Wu HJ, Wang ZF, Tao BB, Wang WW, Zhu YC. Hydrogen sulfide targets the cys320/cys529 motif in kv4.2 to inhibit the Ito potassium channels in cardiomyocytes and regularizes fatal arrhythmia in myocardial infarction. *Antioxid Redox Signal*. 2015;23(2):129–147.
- Calvert JW, Elston M, Nicholson CK, Gundewar S, Jha S, Elrod JW, Ramachandran A, Lefer DJ. Genetic and pharmacologic hydrogen sulfide therapy attenuates ischemia-induced heart failure in mice. *Circulation*. 2010;122(1):11–19.
- Calvert JW, Jha S, Gundewar S, Elrod JW, Ramachandran A, Pattillo CB, Kevil CG, Lefer DJ. Hydrogen sulfide mediates cardioprotection through Nrf2 signaling. *Circ Res*. 2009;105(4):365–374.
- Zanardo RC, Brancaleone V, Distrutti E, Fiorucci S, Cirino G, Wallace JL. Hydrogen sulfide is an endogenous modulator of

- leukocyte-mediated inflammation. *FASEB J.* 2006;20(12):2118–2120.
27. Djordjevic VB, Zvezdanovic L, Cosic V. [Oxidative stress in human diseases]. *Srp Arh Celok Lek.* 2008;136(Suppl 2):158–165.
28. Zinszner H, Kuroda M, Wang X, Batchvarova N, Lightfoot RT, Remotti H, Stevens JL, Ron D. CHOP is implicated in programmed cell death in response to impaired function of the endoplasmic reticulum. *Genes Dev.* 1998;12(7):982–995.
29. Liu T, Zhou Y, Liu YC, Wang JY, Su Q, Tang ZL, Li L. Coronary microembolization induces cardiomyocyte apoptosis through the LOX-1-dependent endoplasmic reticulum stress pathway involving JNK/P38 MAPK. *Can J Cardiol.* 2015;31(10):1272–1281.
30. Ryoo HD. Long and short (timeframe) of endoplasmic reticulum stress-induced cell death. *FEBS J.* 2016;283(20):3718–3722.
31. Hotchkiss RS, Strasser A, McDunn JE, Swanson PE. Cell death. *N Engl J Med.* 2009;361(16):1570–1583.
32. Yu Y, Sun G, Luo Y, Wang M, Chen R, Zhang J, Ai Q, Xing N, Sun X. Cardioprotective effects of notoginsenoside R1 against ischemia/reperfusion injuries by regulating oxidative stress- and endoplasmic reticulum stress- related signaling pathways. *Sci Rep.* 2016;2(6):21730.
33. Xu X, Pang J, Chen Y, Bucala R, Zhang Y, Ren J. Macrophage migration inhibitory factor (MIF) deficiency exacerbates aging-induced cardiac remodeling and dysfunction despite improved inflammation: role of autophagy regulation. *Sci Rep.* 2016;3(6):22488.
34. Klionsky DJAK, Abe A, Abedin MJ, Abeliovich H, Acevedo Arozena A, Adachi H, Adams CM. Guidelines for the use and interpretation of assays for monitoring autophagy (3rd edition). *Autophagy.* 2016;12(1):1–222.
35. Lockshin RA, Zakeri Z. Programmed cell death and apoptosis: origins of the theory. *Nat Rev Mol Cell Biol.* 2001;2(7):545–550.
36. Leist M, Jaattela M. Four deaths and a funeral: from caspases to alternative mechanisms. *Nat Rev Mol Cell Biol.* 2001;2(8):589–598.
37. Szabo C, Papapetropoulos A. Hydrogen sulphide and angiogenesis: mechanisms and applications. *Br J Pharmacol.* 2011;164(3):853–865.
38. Szabo C. Hydrogen sulphide and its therapeutic potential. *Nat Rev Drug Discov.* 2007;6(11):917–935.
39. Papapetropoulos A, Pyriochou A, Altaany Z, Yang G, Marazioti A, Zhou Z, Jeschke MG, Branski LK, Herndon DN, Wang R, Szabo C. Hydrogen sulfide is an endogenous stimulator of angiogenesis. *Proc Natl Acad Sci USA.* 2009;106(51):21972–21977.
40. Cai WJ, Wang MJ, Moore PK, Jin HM, Yao T, Zhu YC. The novel proangiogenic effect of hydrogen sulfide is dependent on Akt phosphorylation. *Cardiovasc Res.* 2007;76(1):29–40.
41. Calvert JW, Jha S, Gundewar S, Elrod JW, Ramachandran A, Pattillo CB, Kevil CG, Lefer DJ. Hydrogen sulfide mediates cardioprotection through Nrf2 signaling. *Circ Res.* 2009;105(4):365–374.
42. Fisher CD, Augustine LM, Maher JM, Nelson DM, Slitt AL, Klaassen CD, Lehman-McKeeman LD, Cherrington NJ. Induction of drug-metabolizing enzymes by garlic and allyl sulfide compounds via activation of constitutive androstane receptor and nuclear factor e2-related factor 2. *Drug Metab Dispos.* 2007;35(6):995–1000.